Journal of Controlled Release 382 (2025) 113677

Contents lists available at ScienceDirect

Journal of Controlled Release

journal homepage: www.elsevier.com/locate/jconrel

Design of lipid-based formulations for oral delivery of a BASP1 peptide targeting MYC-dependent gastrointestinal cancer cells

Dennis To [a], Christian Steinbring [a], Leonie I. Weber [b], Fabrizio Ricci [a,c], Ilaria Polidori [a], Annika Postina [a], Markus Hartl [b,*], Andreas Bernkop-Schnürch [a,*]

[a] Center for Chemistry and Biomedicine, Department of Pharmaceutical Technology, Institute of Pharmacy, University of Innsbruck, Innrain 80/82, 6020 Innsbruck, Austria
[b] Institute of Biochemistry and Center for Molecular Biosciences, University of Innsbruck, Innrain 80/82, 6020 Innsbruck, Austria
[c] Thiomatrix Forschungs- und Beratungs GmbH, Trientlgasse 65, 6020 Innsbruck, Austria

ARTICLE INFO

Keywords:
Oral peptide delivery
Nanoemulsion
Cancer
Oncoprotein
Tumor suppressor
Transcription factor

ABSTRACT

Hypothesis: Oral delivery of the proliferation-inhibiting brain acid-soluble protein 1 effector domain peptide (Myr-NT) towards MYC-dependent gastrointestinal tumors can be achieved by forming hydrophobic ion pairs (HIPs) and incorporating them into lipid-based formulations.
Experiments: Hydrophobic ion pairing of fluorescently-labelled Myr-NT (Myr-NT-TAMRA) was performed, increase in lipophilicity was assessed, and the most promising HIP was subsequently incorporated into a nanoemulsion. Stability of the peptide towards degradation by trypsin was evaluated. Anti-proliferative and anti-invasive measurements were performed upon application of the loaded nanoemulsion on various MYC-dependent human cancer cell lines. Cellular uptake and molecular effect were complementary investigated by confocal laser scanning microscopy (CLSM) and by immunoblot analyses, respectively.
Findings: HIPs of Myr-NT-TAMRA exhibited up to 10,000-fold increase in lipophilicity, thereby enabling incorporation into a nanoemulsion. The formulation significantly boosted stability of incorporated peptide towards enzymatic degradation by trypsin. Furthermore, anti-proliferative measurements on human cancer cell lines revealed superior biological activity of the loaded nanoemulsion compared to the native peptide particularly in lymphoma cells, but also in colorectal cancer cells. Thereby, a correlation with proliferation inhibition as well as differences in MYC protein expression were observed. Finally, CLSM imaging revealed up to 15-fold increased cellular uptake of Myr-NT-TAMRA from the nanoemulsion confirming efficient intracellular delivery of the peptide.
Conclusion: Myr-NT can be efficiently delivered into intestinal tumor cells using orally administered lipid-based formulations.

1. Introduction

Due to their unique properties, peptides are highly sought-after as therapeutic agents, demonstrating significant efficacy against various conditions, including cancer. Among these, MYC-inhibiting peptides have garnered particular interest, as the oncogenic transcription factor MYC (c-Myc) is recognized as a major driver of tumor development [1–5]. MYC is positioned in the centre of a gene regulatory network controlling fundamental cellular processes [4,6], and binds to multiple proteins in order to execute its pleiotropic functions [7,8]. Hence, it is not surprising that numerous attempts have been performed to inhibit MYC's oncogenic activities [5,9]. Examples for MYC-inhibiting peptides are the dominant negative Omomyc interfering with MYC/MAX dimerization and DNA binding [10] and being currently in clinical trials, or the effector domain (ED) of the brain acid-soluble protein 1 (BASP1) [11]. BASP1 was originally identified as a neuronal signalling protein [12] interacting with multiple proteins including calmodulin (CaM) [12–15]. Previous research has shown that the BASP1 gene is transcriptionally downregulated by MYC, and that ectopic expression of BASP1 inhibits MYC-transcription [16] and MYC-dependent cell

This article is part of a Special issue entitled: 'Oral (poly)peptide delivery' published in Journal of Controlled Release.

* Corresponding authors.
E-mail addresses: markus.hartl@uibk.ac.at (M. Hartl), andreas.bernkop@uibk.ac.at (A. Bernkop-Schnürch).

https://doi.org/10.1016/j.jconrel.2025.113677
Received 11 January 2025; Received in revised form 26 March 2025; Accepted 31 March 2025
Available online 2 April 2025

transformation [11,17]. Although BASP1 does not physically interact with MYC, it binds to MYC's interaction partner CaM [18]. Excess BASP1 displaces MYC from CaM, resulting in enhanced MYC proteolysis [11]. Mutational analysis has revealed that a small myristoylated N-terminal region encompassing the BASP1 ED suffices to inhibit MYC-induced cell transformation [11,17]. Additionally, the delivery of a myristoylated BASP1 ED peptide (Myr-NT) has shown potent and specific anti-proliferative effects in several MYC-dependent human cancer cell lines [11].

For the treatment of gastrointestinal cancers, such as gastric and colorectal cancers, direct application of Myr-NT to affected epithelial cells would be most effective. However, Myr-NT is rapidly degraded by proteolytic enzymes in the gastrointestinal tract and is both too hydrophilic and too large to efficiently permeate the cellular membrane of target epithelial cells. To date, this has rendered topical treatment of the gastrointestinal mucosa with Myr-NT impractical.

This study aims to overcome these challenges by developing lipid-based formulations of Myr-NT capable of bypassing enzymatic degradation and cellular membrane barriers [19]. To achieve this, lipophilic complexes of Myr-NT were formed through hydrophobic ion pairing with sodium dodecyl sulfate, sodium dodecyl benzene sulfonate, and sodium docusate. The most lipophilic complexes were then incorporated into nanoemulsions, specifically self-emulsifying drug delivery systems (SEDDS), which are designed to provide protection against proteolytic degradation [20] and enhance cellular uptake [21]. The protective capacity of the oily nanodroplets formed during emulsification was tested against trypsin, a representative gastrointestinal protease. To demonstrate that the therapeutic peptide reaches its intracellular target in an active form, the impact of these formulations on Myr-NT uptake by various cancer cell lines, including the colon cancer cell line SW480, was assessed. Subsequent MYC inhibition was evaluated through cell proliferation assays, cell invasion assays, immunoblotting, and confocal laser scanning microscopy imaging.

2. Materials and methods

2.1. Materials

Fluorescently-labelled Myr-NT (myristoyl-GGKLSKKKKGK-TAMRA-COOH, M_r = 1780.6) and the unlabelled Myr-NT peptide (myristoyl-GGKLSKKKKG-OH, M_r = 1240.3) were commercially synthesized by the company PANATecs (Heilbronn, Germany). Lumogen Yellow (LGY) was a gift from BASF (Ludwigshafen, Germany). Lyso-Phosphatidylcholin was a gift from Lipoid GmbH (Ludwigshafen, Germany). Glyceryl monocaprylate (trade name: Capmul MCM C8) was provided as a free sample from Abitec Corporation (Columbus, OH, USA). Propylene glycol monocaprylate (trade name: Capryol 90) was a free sample from Gattefossé SAS (Lyon, France). Propylene glycol dicaprylate/dicaprate (trade name: Miglyol 840) was kindly donated by IOI Oleo GmbH (Hamburg, Germany). Human erythrocyte concentrate was kindly provided by Tirol Kliniken GmbH (Innsbruck, Austria). Docusate sodium (DS) and soybean oil were purchased from Alfa Aesar (Kandel, Germany). Opti-MEM was obtained from Thermo Fisher Scientific (Vienna, Austria). Hoechst 33528 was purchased from Santa Cruz Biotechnology (Dallas, TX, USA). Acetonitrile (ACN), calcium chloride ($CaCl_2$), dimethyl sulfoxide (DMSO), glucose anhydrous, 4-(2-hydroxyethyl)-1-piperazineethanesulfonic acid (HEPES), isopropylmyristate, methanol, octanol, PEG (20) – sorbitan monooleate (trade name: Tween 80), PEG (35) – castor oil (trade name: Kolliphor EL), potassium chloride (KCl), sodium chloride (NaCl), sodium dodecyl sulfate (SDS), sodium dodecyl benzene sulfonate (SDBS), trifluoroacetic acid (TFA), tris(hydroxymethyl)aminomethane (TRIS), trypsin from porcine pancreas (0.1 mg/mL) and Triton X-100 were purchased from Sigma-Aldrich (Vienna, Austria). DPBS and the cell culture media DMEM, RPMI, and Leibovitz's L-15 medium were purchased from PAN-Biotech (Aidenbach, Germany). Trypsin-EDTA (0.25 %) and glutamine were purchased from Life Technologies (Carlsbad, CA, USA), and Eximus Fetal Bovine Serum (FBS) from Catus Biotech (Tutzing, Germany). Glutaraldehyde was obtained from Merck (Darmstadt, Germany), and acrylamide (Rotiphorese) from Carl Roth (Karlsruhe, Germany).

2.2. HPLC quantification

An HPLC system (Hitachi LaChromElite) with a X Bridge C18 column (250 × 4.6 mm, 5 μm) at 40 °C was used for the quantification of Myr-NT-TAMRA. A gradient method at a flow rate of 1 mL/min was applied as summarized in Table 1 and detection of the peptide occurred at 210 nm. A calibration curve of the peptide was established in methanol.

2.3. Cell culture

The following human cells were obtained from the American Type Culture Collection (ATCC, Manassas, VA, USA): the lymphoblast cell line K562 (CCL-243) from chronic myelogenous leukaemia, the T lymphoblast cell line MOLT4 (CRL-1582) from acute lymphoblastic leukaemia, and the large intestine cell line SW480 (CCL-228) from Dukes C colorectal cancer. Cells were kept mycoplasma-free, which was routinely controlled by polymerase chain reaction (PCR) using the primer pair 5′-GGGAGCAAACAGGATTAGATACCCT-3′/5′-TGCACCATCTGT-CACTCTGTTAACCTC 3′. All cell lines had a passage number < 20 at the time of the respective experiment. K562 and MOLT4 cells were cultured in suspension using RPMI medium supplemented with 10 % (v/v) fetal bovine serum (FBS), and the adherently growing SW480 in DMEM supplemented with glutamine and 10 % (v/v) FBS. All cell lines were grown at 37 °C in a water-saturated 5 % CO_2 atmosphere and their cultivation was carried out as described previously [11]. For peptide transfer mediated by nucleofection, SW480 cells were cultivated in the original Leibovitz L-15 medium supplemented with 10 % (v/v) FBS using a water-saturated atmosphere but no additional CO_2.

2.4. Formation of hydrophobic ion pairs (HIPs)

Hydrophobic ion pairing was initially performed to increase the lipophilicity of Myr-NT-TAMRA and facilitate incorporation into lipid-based formulations [22,23]. The efficacy of three different surfactants, namely SDS, SDBS and DS was assessed for HIP formation with Myr-NT-TAMRA via the organic solvent-free method [24]. Therefore, Myr-NT-TAMRA was dissolved in a concentration of 1 mg/mL in 0.01 M HCl, while the surfactants were dissolved in 0.01 M HCl in concentrations corresponding to molar ratios of 3:1, 6:1 and 12:1 (charge ratio 0.5:1, 1:1 and 2:1, respectively) in relation to Myr-NT-TAMRA. Afterwards, 500 μL of each surfactant solution was dropwise added to 500 μL Myr-NT-TAMRA while stirring at 400 rpm, 25 °C on a thermomixer (ThermoMixer®, Eppendorf, Germany). The samples were incubated for 15 min and then centrifuged for 10 min at 13,400 rpm. The supernatants were withdrawn, while the remaining precipitate was washed two times with demineralized water, lyophilized and stored at −20 °C. 20 μL of each collected supernatant were subjected to HPLC quantification as described above to quantify the amount of unprecipitated peptide. Precipitation efficiency was calculated according to Eq. (1):

$$\textit{Precipitation Efficiency}\ (\%) = \frac{0.5\ \frac{\text{mg}}{\text{mL}} - c\ (\textit{supernatant})}{0.5\ \frac{\text{mg}}{\text{mL}}} \times 100\% \quad (1)$$

Table 1
Parameters of the applied gradient method.

Time [min]	Water + 0.1 % TFA [v/v %]	ACN + 0.1 % TFA [v/v %]
0.0	80	20
8.0	20	80
12.0	80	20
15.0	80	20

2.5. LogP determination

Lipophilicity of the formed HIPs was assessed by determination of the distribution coefficient octanol/water (logP) [25]. Accordingly, 500 µL of demineralized water and 500 µL of octanol were added to each ion pair and vortexed thoroughly. Afterward, the samples were incubated at 300 rpm, 37 °C on a thermomixer for 24 h. Subsequently, the samples were centrifuged for 10 min at 12,500 rpm. 100 µL of each phase were withdrawn, diluted with 400 µL of methanol and subjected to HPLC quantification. LogP was determined using Eq. (2):

$$logP = log\frac{c(octanol\ phase)}{c(water\ phase)} \quad (2)$$

In case of absence of any elution peak in either the octanol or the water phase, the detection limit was used to calculate the corresponding logP.

2.6. Gel electrophoretic evaluation of peptide integrity

Tricine sodium dodecylsulfate polyacrylamide gel electrophoresis (Tricine-SDS-PAGE) [26] was performed to confirm the integrity of Myr-NT, and of Myr-NT-TAMRA peptides after HIP formation. The separating gel was prepared by mixing 10 mL of 3× gel buffer, 17 mL of 30 % acrylamide (AA)/0.8 % bisacrylamide (BIS), 3 mL glycerol (50 °C), 10 µL tetramethylethylenediamine (TEMED) and 100 µL 10 % ammonium peroxodisulfate (APS). The spacer gel consisted of 2 mL 3× gel buffer, 0.6 mL of glycerol, 2 mL of 30 % AA/0.8 % BIS, 1.4 mL of H_2O, 3 µL of TEMED and 30 µL of 10 % APS. The sample gel comprised 1.7 mL of 30 % AA/0.8 % BIS, 4 mL of 3× gel buffer, 6.3 mL of H_2O, 9 µL of TEMED and 90 µL of 10 % APS. Accordingly, HIPs of SDS, SDBS and DS with Myr-NT in a molar ratio of 6:1 (charge ratio 1:1) were prepared as described above. The lyophilized samples were dissolved in a concentration of 0.25 mg/mL in DMSO. As a control, unmodified Myr-NT-TAMRA was dissolved in a concentration of 0.25 mg/mL in demineralized water. 7.5 µL of each solution were subsequently diluted with 2.5 µL of electrophoresis buffer A, before adding the mixtures to the gel. An ultra-low protein marker (Merck, Darmstadt, Germany) showing bands in the range between 26,600 Da and 1,060 Da was added to the gel. The loaded gel was run at constant 20 mA in an electrophoresis chamber for 24 h. Afterward, the gel was washed for 10 min in deionized water and fixed with 5 % (m/v) glutaraldehyde solution for 1 h at room temperature. Subsequently, the gel was rinsed trice with water and stained for 1 h with a 0.025 % (m/v) Coomassie Brilliant Blue in aqueous 10 % (v/v) acetic acid solution followed by de-staining for >24 h.

2.7. Development and formation of nanoemulsions

Three nanoemulsion candidates for the delivery of the Myr-NT-TAMRA-HIPs were developed. Their respective composition is listed in Table 2.

Table 2
Composition of the developed nanoemulsions.

	F1 (v/v %)	F2 (v/v %)	F3 (m/m %)
Lipids			
Glyceryl monocaprylate	30		40
Isopropylmyristate	40		
Propylene glycol dicaprylate/dicaprate			30
Propylene glycol monocaprylate		40	
Soybean oil		30	
Surfactants			
Lyso-Phosphatidylcholin			30
PEG (20) – sorbitan monooleate	30		
PEG (35) – castor oil		30	

For preparation of the nanoemulsions, excipients were added in the indicated ratios in an Eppendorf Tube. F1 and F2 were then heated to 37 °C, whereas F3 was melted at 90 °C. Subsequently, all formulations were stirred at the indicated temperature at 2,000 rpm with a thermomixer and then vortexed. Afterward, the preconcentrates were diluted to a concentration of 0.2 % (v/v) in HEPES-buffered saline solution pH 7.4 (HBS, containing 1 g/L glucose, 20 mM HEPES, 5 mM KCl, 136.7 mM NaCl and 1 mM $CaCl_2$) and vortexed. F3 was ultrasonicated by 20 short ultrasonication pulses with a probe sonicator (Hielscher UP200Ht, Hielscher Ultrasonics GmbH, Teltow, Germany). Samples for size and polydispersity index (PDI) measurements were subsequently diluted in HBS to a final concentration of 0.02 %, while samples for zeta potential measurement were diluted in demineralized water, to limit interference of ionic strength with the measurement. Particle size, PDI and zeta potential were measured with a Zeta Sizer (Malvern Panalytical, Malvern, UK) by dynamic and electrophoretic light scattering.

2.8. Cytocompatibility assays

2.8.1. Evaluation of hemotoxic potential

Membrane and blood toxicity of the nanoemulsions were evaluated by a hemolysis assay using a human erythrocyte concentrate [27,28]. For this, the formulations F1-F3 were prepared in concentrations of 0.2 %, 0.1 %, 0.05 % and 0.02 % (v/v) in HBS. Triton X-100 in a concentration of 0.1 % (m/v) and HBS served as positive and negative controls, respectively. The erythrocyte concentrate was diluted 1:200 with HBS, and subsequently 250 µL of the diluted erythrocyte suspension were added to 250 µL of the prepared formulations resulting in final formulation concentrations of 0.1 %, 0.05 %, 0.025 % and 0.01 % (v/v). The samples were incubated for 24 h at 37 °C under shaking at 100 rpm. Afterward, the samples were centrifuged for 10 min at 500 ×*g* and absorbance of the supernatant was measured at 415 nm using a multi-well plate reader (Tecan Spark™, Tecan Trading AG, Switzerland).

2.8.2. Evaluation of cytotoxicity

An initial cytotoxicity screening for the developed formulations was carried out via cell proliferation assay on the adherent model cell line SW480. For this reason, cells were seeded in a sterile 24-well plate in a concentration of 5×10^4 cells per well in a total volume of 500 µL DMEM supplemented with 10 % (v/v) heat-inactivated FBS. The plate was incubated overnight at 37 °C, 95 % relative humidity, and 5 % CO_2 to allow cells to attach to the well. The next day, the oily preconcentrates were emulsified in HBS and subsequently diluted to a final concentration of 0.01 % in serum-supplemented DMEM. The cell supernatant was aspirated and 500 µL aliquots of the diluted formulations were added to each well of the plate. A 4:1 serum supplemented DMEM/HBS mixture was used as blank, to evaluate the proliferation behaviour in the absence of xenogenic substances. The plate was incubated in an Incucyte S3 Life cell analysis system (Essen Bioscience Inc., Ann Arbor, MI, USA) at 37 °C for 48 h and 9 images of each well were automatically taken in 2 h intervals in a 10× magnification. Afterward, an AI-based algorithm was used to determine the cell count in each well.

2.9. Development of loaded nanoemulsions and stability assessment

The most promising formulation was selected based on the results of the formulation screening and cytotoxicity assessment. In order to obtain the loaded formulation, HIP of Myr-NT-TAMRA was dissolved in the formulation preconcentrate in a concentration of 3 % (m/m) by continuous agitation with a thermomixer at 1,700 rpm at 25 °C. Complete dissolution was indicated by the absence of a precipitate after centrifugation and a homogenously coloured preconcentrate. The preconcentrate was subsequently emulsified in a concentration of 0.02 % (v/v) in either HBS, for size and PDI measurement, or water, for zeta potential determination. The formed emulsions were incubated at 37 °C for 24 h at a thermomixer, while shaking at 500 rpm and the

measurements were performed after 0 h, 4 h and 24 h of incubation to assess time-dependent stability of the formed emulsions. The characterized preconcentrates were stored at −20 °C until further use.

2.10. Enzymatic degradation studies

Native peptide and loaded formulation were subjected to an enzymatic degradation study with trypsin as previously described [20]. Myr-NT-TAMRA was dissolved in a concentration of 0.6 mg/mL in protease buffer pH 6.8 (100 mM TRIS, 2 mM $CaCl_2$), while the loaded formulation was diluted 1:50 in the same buffer. 150 μL of each sample was mixed with 150 μL of trypsin solution (0.1 mg/mL) and incubated in a thermomixer at 37 °C while stirring at 300 rpm for 1 h. A 100 % control was performed by the addition of pure protease buffer pH 6.8 to the unmodified peptide solution. At predetermined time points, 25 μL aliquots were withdrawn and mixed with 50 μL of methanol + 0.5 % (v/v) TFA to stop the enzymatic reaction. The aliquots were subsequently subjected to HPLC analysis as described above to determine the amount of non-cleaved peptide.

2.11. Cell proliferation measurements

Anti-proliferative effects of the native Myr-NT-TAMRA and Myr-NT-TAMRA-loaded nanoemulsions were assayed using above indicated human cancer cell lines. Thereby, the amount of loaded peptide in 0.025 % (v/v) or 0.0185 % (v/v) nanoemulsions corresponds to 4 μM or 3 μM of Myr-NT-TAMRA, respectively. For SW480, each 125,000 cells were seeded into the wells of an MP12 plate and incubated overnight. Then, the medium was replaced with 500 μL serum-free DMEM, followed by the addition of each 500 μL serum-free DMEM containing 6 μM free Myr-NT-TAMRA, loaded nanoemulsion 0.037 % (v/v) or empty nanoemulsion 0.037 % (v/v) resulting into final concentrations of 3 μM or 0.0185 %, respectively. For K562 and MOLT4, each 125,000 cells suspended in 500 μL serum-free RPMI medium were transferred into the wells of an MP12 plate. Then, each 500 μL serum-free medium were added containing 8 μM (K562) or 6 μM (MOLT4) of Myr-NT-TAMRA resulting in final concentrations of 4 μM or 3 μM, respectively. Likewise, each 500 μL of serum-free medium containing a Myr-NT-TAMRA-loaded nanoemulsion, or the empty nanoemulsion were added, resulting in final concentrations of 0.025 % (v/v) (K562) or 0.0185 % (v/v) (MOLT4).

Cells with administered peptides were incubated for 4 h. Then, the medium was replaced by each 1 mL of the appropriate medium containing 10 % (v/v) FBS. For this, cells grown in suspension were centrifuged at 6,000 rpm for 5 min, then the supernatant was withdrawn and cells were resuspended in culture medium. Cells were incubated for 3–4 d and then cell numbers determined in triplicate using a Coulter Counter (Beckman Coulter, Brea, CA, USA).

For peptide delivery by electroporation (nucleofection), each 1.33×10^6 SW480 cells were suspended in 100 μL of Nucleofector solution V (Lonza, Basel, Switzerland) and mixed with Myr-NT resulting into an initial concentration of 20 μM. Nucleofection was done as described previously [17] using the program L-24 and cells were subsequently plated onto the wells of an MP6 plate resulting in a final peptide concentration of 1 μM. After incubation for 2 d, cells were counted and protein extracts prepared.

2.12. Cell invasion assay

Invasion through an extracellular matrix (ECM) was determined using the ECM550 cell invasion assay kit from Merck (Darmstadt, Germany). MOLT4 cells were treated for 4 h with Myr-NT-TAMRA-loaded nanoemulsion, or the empty nanoemulsion as described under 2.11. Then, each 300,000 cells suspended in 300 μL serum-free RPMI were added into the upper invasion chamber containing a rehydrated ECM. The assembly was subsequently placed onto the lower chamber consisting of an MP24 well filled with 500 μL RPMI containing 10 % (v/v) FBS. After 72 h incubation at 37 °C, cells having passed the ECM and growing in suspension in the lower chamber medium were counted.

2.13. Immunoblot analysis

Protein extracts from cells were prepared 4 h after peptide delivery as described [29], or 2 d after nucleofection [11]. SDS-PAGE and immunoblotting were carried out as previously described [17,18] using antibodies directed against human MYC (D3N8F, Cell Signaling, Danvas, MA, USA), tubulin α (T5168, Sigma-Aldrich, St. Louis, MO, USA), or GAPDH (#AB8245, Abcam, Cambridge, UK). For densitometry, relative protein levels were determined using the program Image-Quant TL (GE Healthcare Technologies, Chicago, IL, USA) as described previously [18].

2.14. Confocal laser scanning microscopy imaging (CLSM)

CLSM was performed to investigate the cellular internalisation of the loaded nanoemulsion [30] and the TAMRA-labelled peptide [31]. Prior to CLSM, absorbance and emission spectra of Myr-NT-TAMRA, Myr-NT-TAMRA-HIP and Myr-NT-TAMRA loaded nanoemulsion were recorded in the wavelength range 450 nm – 650 nm to evaluate a possible impact of the formulation on fluorescence characteristics of Myr-NT-TAMRA. For this, Myr-NT-TAMRA was dissolved in a concentration of 0.1 mg/mL in HBS, whereas Myr-NT-TAMRA-HIP stock solution in DMSO (1 %, m/v) was diluted in HBS to the same concentration. The preconcentrate of the Myr-NT-TAMRA loaded nanoemulsion was emulsified in a 1:300 dilution in HBS (v/v) corresponding to a concentration of Myr-NT-TAMRA of 0.1 mg/mL. Excitation of all samples was performed at 500 nm with equal gain for every well.

For CLSM, the lipid phase was additionally labelled with LGY in a concentration of 0.05 % (m/v) and fluorescence emission spectra of the particles (excitation wavelengths 405 and 488 nm) were compared with Myr-NT-TAMRA to exclude a potential overlap of both fluorophores.

2.14.1. Cellular uptake in SW480 cells

SW480 cells were seeded two d prior to the experiment in a concentration of 4×10^4 cells per well in a final volume of 180 μL of DMEM + 10 % (v/v) FBS in an 8-well ibidi glass slide (ibidi, Gräfelfing, Germany). The plate was incubated for 2 d at 37 °C, in an atmosphere of 5 % CO_2 and 100 % relative humidity. At the day of the experiment, the supernatant was carefully removed, replaced with 180 μL of Opti-MEM and the plate was incubated for 30 min at 37 °C. Afterward, the supernatant was withdrawn and 180 μL of LGY- labelled Myr-NT-TAMRA loaded formulation in a concentration of 0.02 % (m/v), or unmodified Myr-NT-TAMRA in a concentration of 6 μg/mL (= 3.37 μM) in Opti-MEM, were applied to the cells. The plate was incubated for 4 h at 37 °C. Subsequently, the cells were washed once with Opti-MEM and the nuclei were stained with Hoechst 33528 prior to imaging with the confocal laser scanning microscope Leica TCS SP8 (Leica, Wetzlar, Germany). Image postprocessing was performed utilizing ImageJ: the yz- and xz-projections were prepared from 10 xy-images of an image stack taken at 0.2 μm z-step length. Furthermore, 3D image filtering was conducted using a gaussian and median filter. From the recorded image data, the colocalization between uptaken nanoemulsion and TAMRA was determined using the ObjectFinder-application in MatLab. A minimum of a 50 % overlap of nanoemulsion-objects with the TAMRA-object was counted as colocalized. Cellular uptake was afterwards evaluated using a custom written MatLab program via determining the mean fluorescence intensity per image plane ($<I>_n$) in the TAMRA channel along n = 4 planes in z-direction, from the middle of the cell to the bottom. The average intensity of these 4 planes (I_{Fluo}) was calculated and used as a measure to determine the relative uptake into the cell.

2.14.2. Cellular uptake in K562 and MOLT4 cells

K562 and MOLT4 cells were seeded in a concentration of 4×10^4 cells per well in a final volume of 90 µL of Opti-MEM in an 8-well ibidi glass slide. Subsequently, 90 µL of LGY-labelled Myr-NT-TAMRA loaded formulation in a concentration of 0.04 % (m/v) or unmodified Myr-NT-TAMRA in a concentration of 12 µg/mL (= 6.74 µM) in Opti-MEM were applied to the cells resulting in final concentrations of 0.02 % (m/v) and 6 µg/mL (= 3.37 µM), respectively. The plate was incubated for 4 h at 37 °C. Subsequently, cells were resuspended and each cell suspension was transferred into a 1.5-mL reaction tube and pelleted by centrifugation at 6,000 rpm for 5 min. The cells were washed once with Opti-MEM and the nuclei were subsequently stained with Hoechst 33528 before imaging with the Leica TCS SP8 microscope. Image post-processing and image analysis were performed as described above.

2.15. Statistical data analysis

Unless otherwise indicated, statistical data analysis was performed using one-way ANOVA in combination with Bonferroni post-hoc-test to analyse the significance of differences between means of more than two groups calculated with GraphPad Prism 5.01, while Student's *t*-test was used to compare means of two groups. The level of $p < 0.05$ was set as the minimum level of significance.

3. Results and discussion

3.1. Formation and characterization of the hydrophobic ion pairs

The sequences of the investigated BASP1-effector peptides, namely Myr-NT and the fluorescently labelled Myr-NT-TAMRA derivative are depicted in Fig. 1 (A). Hydrophobic ion pairing was carried out to increase lipophilicity of Myr-NT-TAMRA and to enable subsequent incorporation into lipid-based formulations. As sulfate-, sulfonate- and sulfo-succinate-based counterions proved to be highly effective for hydrophobic ion pairing of several peptides and proteins [32–34], the potential of representatives of these classes, namely SDS, SDBS and DS [Fig. 1 (B)], for the formation of HIPs with Myr-NT-TAMRA was assessed. As depicted in Fig. 1 (C) all three counterions effectively formed HIPs with Myr-NT-TAMRA in a charge ratio of 1:1 (= molar ratio 6:1).

The highest precipitation efficiency was obtained with SDS, reaching almost 100 % of precipitation efficiency, followed by SDBS (90 %) and DS (78 %). Applying either a lower (0.5:1) or a higher (2:1) charge ratio led to major decreases in precipitation efficiency for all three counterions, indicating that 1:1 is the optimum ratio for hydrophobic ion pairing with Myr-NT-TAMRA. This is in good agreement with literature reports on hydrophobic ion pairing of peptides and proteins with anionic counterions [25,34,35]. It is suggested that an excess of counterion leads to the formation of micelles, which are re-solubilizing the formed HIP, thereby hindering complete precipitation [32]. A high precipitation efficiency usually goes along with a high product yield and a more pronounced increase in lipophilicity of the peptide, which is a key property for incorporation into lipid-based formulations [36]. While DS is overall a highly suitable counterion for hydrophobic ion pairing of peptides and proteins, it was less efficient than SDS and SDBS in precipitating Myr-NT-TAMRA out of solution. It is assumed, that its branched, lipophilic structure plays a role in this observation. As four of the total six charges of Myr-NT-TAMRA are sequentially located in close proximity of each other, the bulky DS molecules were likely sterically hindered to occupy all available charges, causing incomplete precipitation.

Fig. 1 (D) shows logP values of the formed Myr-NT-TAMRA-HIPs. The most significant increases in lipophilicity were achieved in a charge ratio of 1:1 with SDS and DS, leading to an overall elevation in logP of 4 units, corresponding to a 10,000-fold increase in lipophilic character of the peptide based on the solubilities in octanol and water. On the other hand, SDBS appeared to be not suitable for acquiring highly

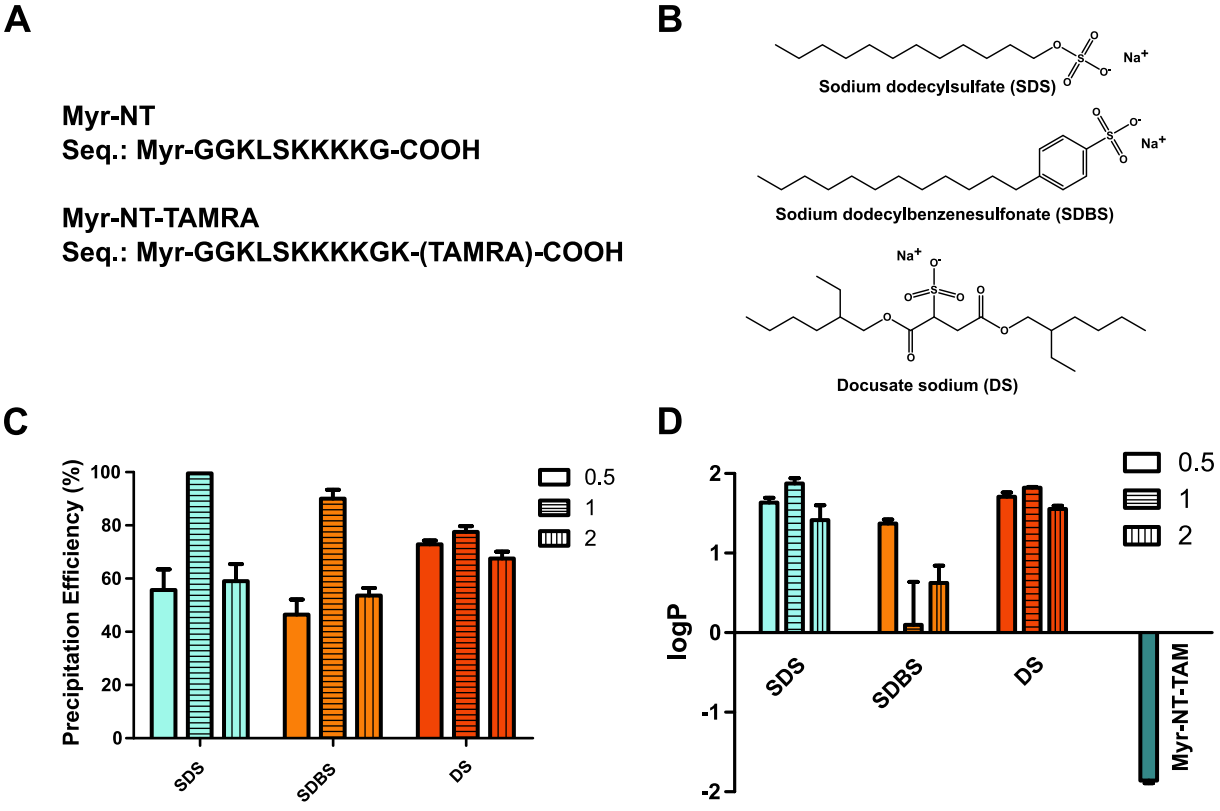

Fig. 1. Sequences of the investigated BASP1-effector peptides **(A)** and the applied counterions for hydrophobic ion pairing of Myr-NT-TAMRA **(B)**. Precipitation efficiency **(C)** and logP of the formed hydrophobic complexes of Myr-NT-TAMRA **(D)**. Data are means ± standard deviation of at least three experiments.

lipophilic ion pairs with Myr-NT-TAMRA, as significantly lower logP values were achieved and the formed products appeared to be less homogenous in their composition, indicated by a high standard deviation for the charge ratio of 1:1. Furthermore, changing the charge ratio to 0.5:1 or to 2:1 decreased the logP of the obtained HIPs for all tested counterions, which is in good agreement with results of precipitation efficiency.

Lastly, a Tricine-SDS-PAGE suitable for peptide separation was carried out, to investigate the impact of hydrophobic ion pairing on the structural integrity of Myr-NT-TAMRA. Fig. S1 (Supplementary Material) visualizes the gel after applying electrophoresis and Coomassie Brilliant Blue staining.

Based on the acquired results, HIPs formed with Myr-NT-TAMRA and SDS in a charge ratio of 1:1 were selected for further studies as they provided the highest lipophilicity with an excellent precipitation efficiency of almost 100 %, while fully preserving the integrity of the Myr-NT-TAMRA peptide.

3.2. Development and characterization of the empty nanoemulsions

Considering the presumed anti-proliferative effect of Myr-NT-TAMRA it was key to develop a formulation that solely served as delivery vehicle, potentially increasing the efficacy of Myr-NT-TAMRA, but did not exhibit any unspecific cytotoxic effects itself. It is known that some compounds of lipid-based formulations, such as surfactants show concentration-dependent cytotoxic effects [37,38]. Therefore, the number of compounds in each formulation was limited to a maximum of three, as each component could cause undesired cellular effects. Furthermore, a simple, scalable production process is favoured. Eventually, three potential formulations were developed based on either non-ionic PEG (20)-sorbitan monooleate, PEG (35) – castor oil or zwitterionic lyso-phosphatidylcholin as a surfactant, as non-ionic and zwitterionic surfactants exhibit significantly less cytotoxicity compared to cationic and anionic charged ones [38]. The composition of the developed formulations, as well as particle size, PDI and zeta potential are visualized in Fig. 2.

As only net non-charged compounds were used, all formulations exhibited an almost neutral zeta potential. F1 and F2 showed particle sizes <100 nm and a PDI < 0.2, whereas F3 showed slightly elevated particle sizes as well as PDI. Furthermore, F1 and F2 showed favourable self-emulsifying properties, whereas F3 needed to be ultrasonicated to acquire a nanoemulsion. In terms of storage stability of peptides and proteins, a self-emulsifying drug delivery system is a major advantage compared to a lipid-based formulation that requires ultrasonication. As the self-emulsifying preconcentrate is water-free, the preconcentrate can be conveniently stored after the incorporation of the drug without the risk of hydrolysis. Furthermore, no additional equipment for the preparation of the emulsion is required, the preconcentrate just needs to be diluted to the desired concentration to obtain the emulsion. Nonetheless, physical particle properties of all three formulations appeared to be suitable for the delivery of Myr-NT-TAMRA. Accordingly, cytotoxicity assays were carried out on the formulations and the least toxic formulation was chosen for further studies. The results are depicted in Fig. 3.

Hemoglobin release studies with human red blood cells can be useful for predicting interactions between nanomaterials and biological membranes [28]. A high release of hemoglobin indicates major lysis of the blood cell, correlating with potentially increased cytotoxicity. Fig. 3 (A) depicts the results of hemolytic activity for all formulations. F1 and F3 caused complete hemolysis in the investigated concentration range of 0.1 to 0.01 %, indicating significant membrane toxicity. In contrast, F2 was non-hemolytic up to a concentration of 0.025 % and only mildly hemolytic in a concentration of 0.05 %. Even in a concentration of 0.1 %, no complete hemolysis was observed. In comparison with literature results, the hemotoxicity of F2 can be rated as relatively low, as multiple non-ionic and zwitterionic nanoemulsions were reported that exhibit major hemotoxicity up to a dilution of 1:20,000 (0.005 %) [39,40]. Complementary to the hemotoxicity assay, an additional dynamic cell proliferation experiment was carried out, to evaluate possible cytotoxic effects of the formulations on the model cell line SW480. Plots of dynamic cell proliferation in the presence of the formulations over an incubation period of 48 h are presented in Fig. 3 (B).

Cells incubated with F2 or F3 showed similar cell proliferation profiles as the cells incubated with medium only, indicating the absence of cytotoxic effects on SW480 in this concentration. However, a significant inhibition of cellular proliferation was observed for F1, as the cell count remained almost constant over the whole incubation period. Live-cell images acquired after 0 d and 2 d of incubation, which are depicted in Fig. 3 (C), confirm that F1 is not reducing the number of viable cells, but inhibiting their proliferative activity in a cytostatic manner. Furthermore, in contrast to images recorded for blank, F2 and F3, no patterns of

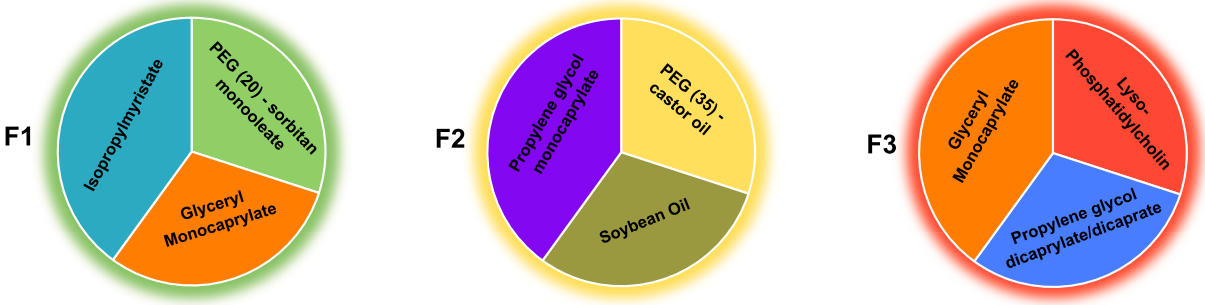

	Size (nm)	PDI	Zeta potential (mV)
F1	52 ± 2	0.12 ± 0.01	-6 ± 0
F2	78 ± 1	0.12 ± 0.01	-3 ± 0
F3	145 ± 7	0.21 ± 0.03	-2 ± 2

Fig. 2. Compositions of formulations F1–F3 with respective particle size, PDI and zeta potential in a concentration of 0.02 % (v/v). Data are means ± standard deviation of at least three experiments.

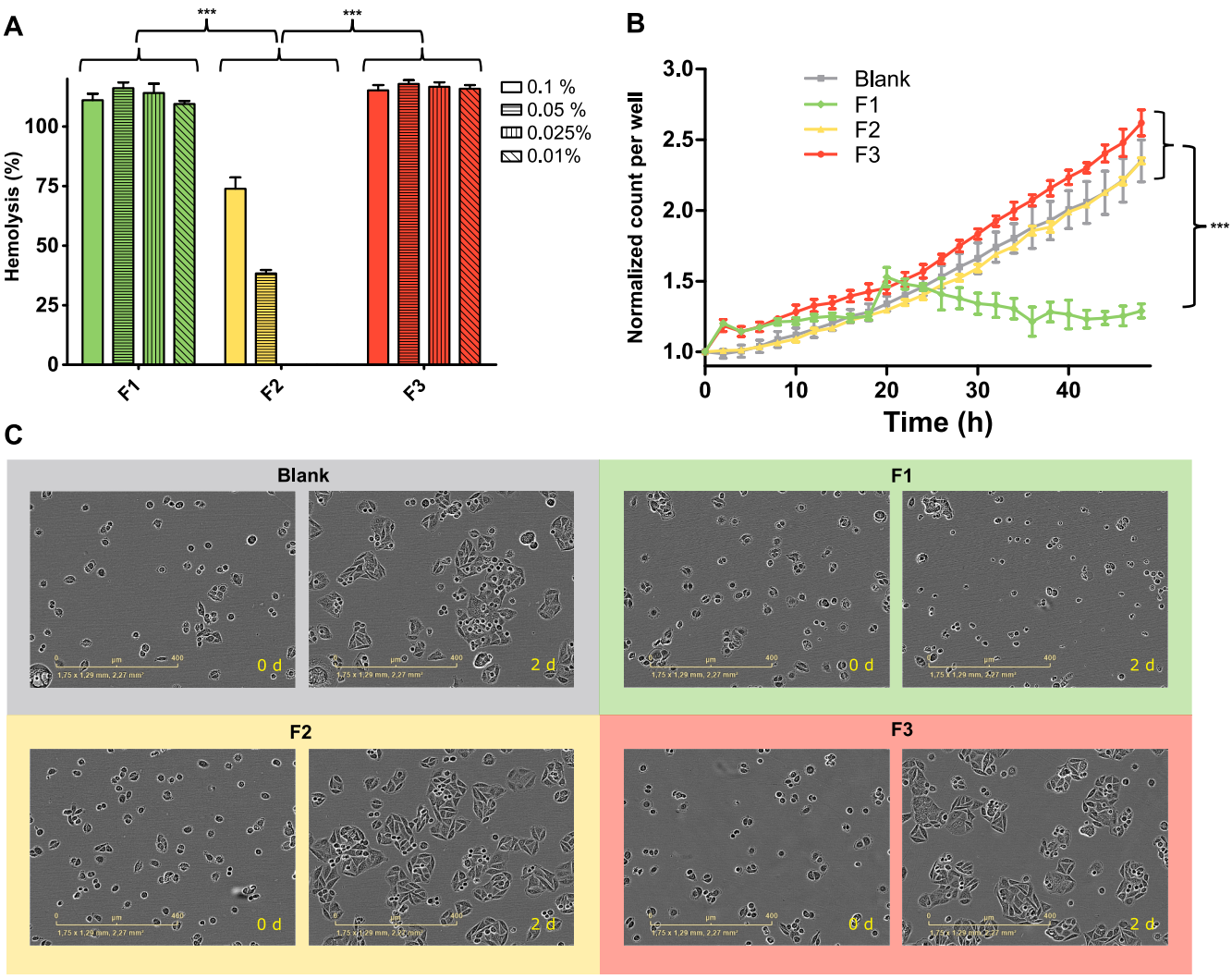

Fig. 3. Hemolytic activity of the formulations in concentrations of 0.1, 0.05, 0.025 or 0.01 % (v/v) **(A)**. Cellular proliferation of SW480 in the presence of the formulations F1-F3 in a concentration of 0.01 % (v/v) **(B)** as well as corresponding Incucyte images **(C)**. Data are means ± standard deviation of at least three experiments. Significant differences are indicated as ***$p < 0.001$.

cell proliferation were visible for F1. Cell bodies of SW480 incubated with F1 were shrunken, but appeared to be alive after 2 d. Nonetheless, a decrease in cell volume is a clear indication for cytotoxicity [41]. It is assumed that PEG (20) - sorbitan monooleate, also known as polysorbate 80, might play a major role in this observation. While this surfactant is generally recognized as safe, literature also suggests slight cytostatic effect of polysorbates on several cell lines [42,43]. As the cells are damaged but remain alive, typical short-term cell viability assays relying on cellular metabolism such as the resazurin, or the MTT assay [44] fail to detect the observed form of cytotoxicity.

Taking the results of hemolytic activity and dynamic cell proliferation into account, formulation F2 was chosen for further studies as it exhibited the lowest membrane toxicity and no undesired, unspecific anti-proliferative effects.

3.3. Stability study

Formulation F2 was loaded with Myr-NT-TAMRA-SDS in a concentration corresponding to 3 % of Myr-NT-TAMRA subsequently designated as F2-MNT. Centrifugation of the preconcentrate showed no precipitate and the content of Myr-NT-TAMRA was verified via HPLC analysis as described above. As the incorporated peptide might influence physical particle characteristics, a stability study over 24 h was performed. The results are shown in Fig. 4.

A slight, but significant change in initial particle size was observed after incorporation of Myr-NT-TAMRA-SDS in F2 (50 nm versus 75 nm). This can likely be attributed to the surfactant structure of Myr-NT-TAMRA, possessing a lipophilic tail and a hydrophilic head group. Therefore, an assembly close to the interface of oil and water is likely, consequently influencing particle size and zeta potential. Only minor changes in particle size were obtained after 4 h, whereas an incubation of 24 h at 37 °C led to an increase in particle size to >100 nm in both cases. Zeta potential of F2 was around −10 mV in water and switched to 2 mV after incorporation of Myr-NT-TAMRA-SDS. The zeta potential of F2 and F2-MNT remained stable over 24 h. Nonetheless, the observed slight differences in zeta potential seem to be negligible, as the measured potentials are close to zero even in demineralized water and the adsorption of electrolytes in medium will likely mask this minor deviation in zeta potential [45]. However, the empty formulation as F2, as well as the loaded formulation F2-MNT, were sufficiently stable for further experiments and data obtained for F2-MNT provided further evidence for the successful incorporation of Myr-NT-TAM-SDS in F2-MNT.

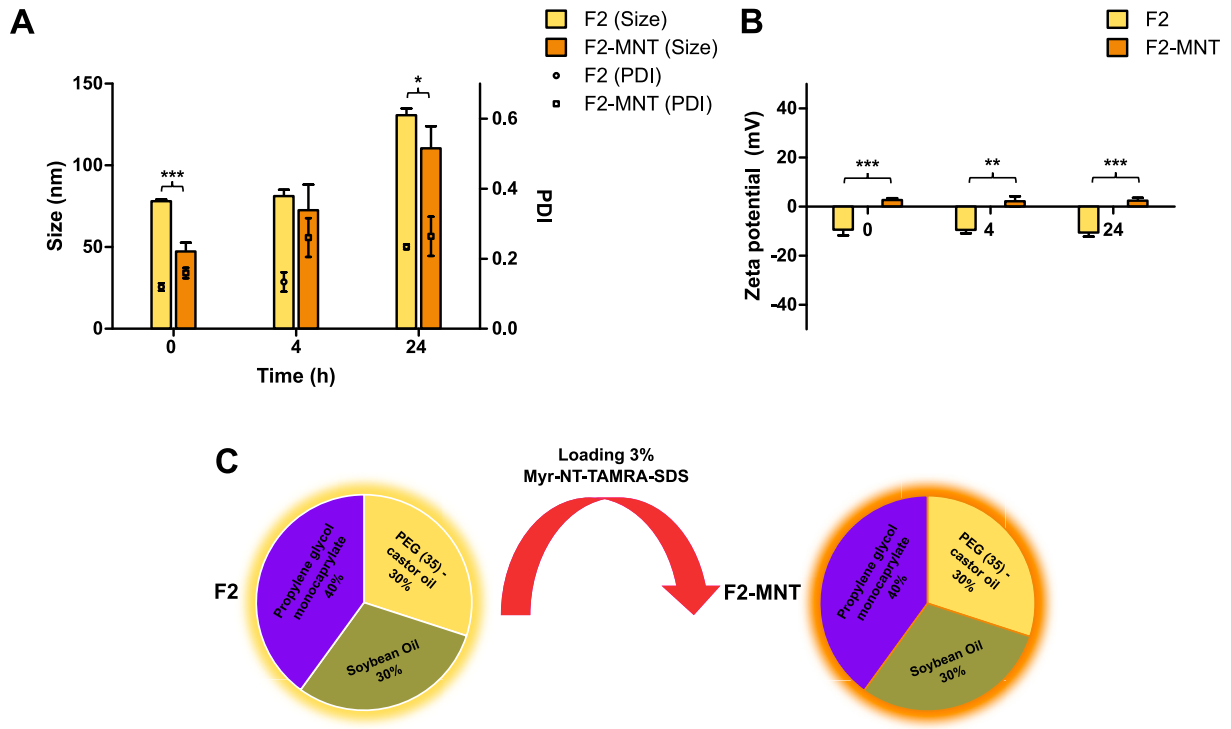

Fig. 4. Changes in particle size, PDI **(A)** and zeta potential **(B)** of F2 and F2-MNT over 24 h at 37 °C. Graphical scheme of the composition of F2 compared to F2-MNT **(C)**. Data are means ± standard deviation of at least three experiments. Significant differences are indicated as *p < 0.05, **p < 0.01 and ***$p < 0.001$.

3.4. Evaluation of protective effect of the nanoemulsions

One major bottleneck for a possible therapeutic application of peptides is their mostly low stability in a bioenvironment. This is mostly a result of enzyme-induced cleavage, leading to degradation of the peptide and loss of activity, thereby diminishing even excellent biological activities. Lipid-based formulations such as nanoemulsions have the potential to protect incorporated cargo from degradation, as enzymes cannot enter the lipophilic phase because of their hydrophilic character [22,23]. As a result, the enzyme has limited access to the cargo and is only able to cleave superficially bound peptide or peptide that was released from the oily droplet. Herein, we used the serine protease trypsin as a model enzyme to investigate if the nanoemulsion can protect Myr-NT-TAMRA from degradation, thus preserving its potential activity. Trypsin is a prominent pancreatic enzyme which is capable of cleaving a wide variety of peptide and protein drugs, thus representing a vital part of the so-called enzymatic barrier of the gastrointestinal system [22].

As shown in Fig. 5, the nanoemulsion provided significant protection against proteolysis of Myr-NT-TAMRA. While the native peptide in aqueous solution was completely cleaved within 5 min, resulting in two peptide fragment peaks (Supplementary Material, Fig. S2), around 50 % of the initial peptide was still intact in the loaded nanoemulsion after 1 h of incubation with trypsin. Compared with the cleavage time of other peptides such as daptomycin (1.6 kDa, >120 min) [46], leuprorelin acetate (1.2 kDa, 120 min) [47] or insulin (5.8 kDa, 60 min) [48], Myr-NT-TAMRA (1.8 kDa, 5 min) is extremely rapidly cleaved by trypsin. This indicates high vulnerability of the peptide towards enzymatic inactivation and highlights the necessity of a formulation for a biomedical application of Myr-NT-TAMRA. Increased resistance against proteolysis requires a sufficiently lipophilic HIP of the peptide, to ensure effective incorporation into SEDDS [36,49]. The ion pairs formed with SDS appeared to be appropriately encapsulated into the SEDDS nanodroplets. However, as the peptide itself exhibits surfactant properties due to its structure, the formed ion pair is likely located to a certain amount close to the interface of the particle, thus allowing trypsin to cleave a fraction of the highly vulnerable peptide. Nonetheless, the achieved protective effect from enzymatic degradation can be considered as major advantage of the nanoemulsion, paving the way for an oral therapeutic application of Myr-NT-TAMRA.

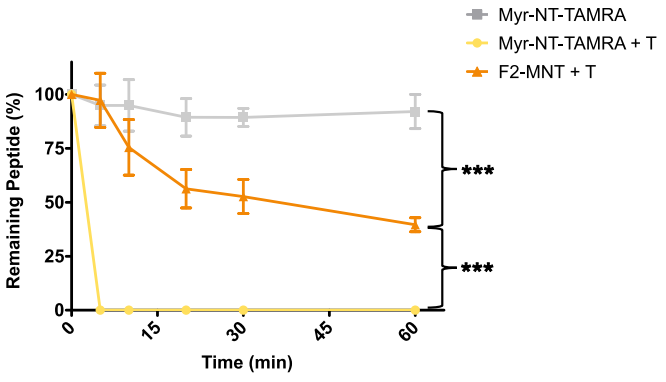

Fig. 5. Enzymatic degradation of Myr-NT-TAMRA and F2-MNT in the presence of trypsin over 1 h. Data are means ± standard deviation of at least three experiments. Significant differences are indicated as ***$p < 0.001$.

3.5. Anti-proliferative effect of the BASP1-effector peptide

To test the F2-MNT nanoemulsion containing the Myr-NT-TAMRA peptide for biological activity, the following human cancer cells were used, which are all featured by high levels of MYC expression: the adherently growing colon cancer cell line SW480, and the leukaemia cell lines K562 and MOLT4, the latter ones growing in suspension (Fig. 6). As controls, the free Myr-NT-TAMRA peptide and the empty nanoemulsion (F2) were applied.

Application of Myr-NT-TAMRA loaded nanoemulsion corresponding to concentrations of 3–4 μM caused a clear reduction in cell proliferation with the most pronounced effect in MOLT4 cells (MOLT4: 6 % < K562: 42 % < SW480: 66 %), which is in accordance with previous results when the BASP1 ED peptide Myr-NT was directly delivered at high

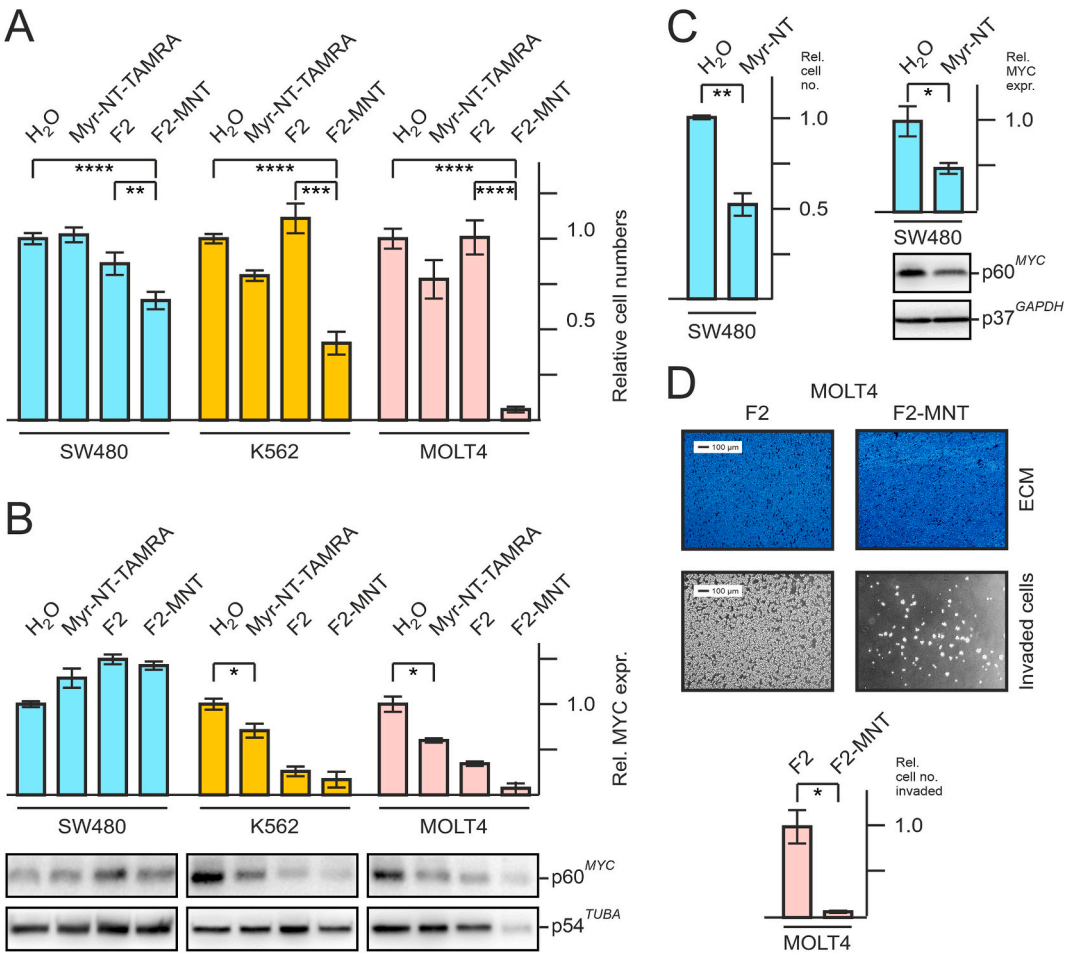

Fig. 6. The cell lines SW480 (turquoise), K562 (orange) and MOLT4 (pink) were incubated for 4 h with Myr-NT-TAMRA or F2-MNT. The final peptide concentrations were 4 μM (K562) or 3 μM (MOLT4, SW480). The solvent (H_2O) or equal amounts of the empty formulation (F2) were used as controls. Cell numbers were determined after 3–4 d incubation. Vertical bars show standard errors of the mean (SEM) from independent experiments (n = 4). Statistical significance was assessed by using an unpaired Student *t*-test (**$p < 0.01$, ***$p < 0.001$, ****$p < 0.0001$) **(A)**. Immunoblot analysis using extracts from cells shown under **(A)** prepared 4 h after peptide addition, and antibodies directed against human MYC or tubulin α (TUBA). The levels (%) of MYC expression were determined using the program ImageQuant TL and are depicted as bars in relation to mock deliveries (H_2O, 100 %). Vertical bars show standard errors of the mean (SEM) from independent experiments (n = 3). Statistical significance was assessed by using an unpaired Student *t*-test (*$p < 0.05$) **(B)**. Determination of SW480 cell proliferation (left panel) and MYC or GAPDH protein expression (right panel) after delivery of the free Myr-NT peptide by nucleofection. Cell numbers were determined and protein extracts were prepared after 2 d. Vertical bars show standard errors of the mean (SEM) from independent experiments (n = 3). Statistical significance was assessed by using an unpaired Student *t*-test (*$p < 0.05$, **$p < 0.01$) **(C)**. Invasion of MOLT4 treated with Myr-NT-TAMRA-containing nanoemulsion (F2-MNT) or the empty formulation (F2) as described under **(A)**. Equal amounts of treated cells were subjected to a cell invasion assay and after 3 d cells crossing the extracellular matrix monitored. Upper panel: stained matrix; middle panel: micrographs of invaded cells; lower panel: relative numbers of invaded cells. Vertical bars show standard deviations (SD) from independent experiments (n = 3). Statistical significance was assessed by using an unpaired Student *t*-test (*$p < 0.05$) **(D)**. (For interpretation of the references to colour in this figure legend, the reader is referred to the web version of this article.)

concentrations into these cells [11]. On the other hand, delivery of the free Myr-NT-TAMRA peptide in low concentrations (3–4 μM) only showed moderate effects in K562 and MOLT4 and even no effect in SW480 [Fig. 6 (A)] demonstrating the efficacy of the nanoemulsion. To test if the BASP1 ED peptide has an impact on the expression of the MYC oncoprotein, like the full-length BASP1 protein does [11], cell extracts were prepared after 4 h of incubation and analysed by immunoblotting using a MYC-specific antibody [Fig. 6 (B)].

Application of the free peptide in low micromolar concentrations showed a clear reduction of MYC protein levels in K562 and MOLT4 cells, whereas no change was observed in SW480, which correlates with the relevant proliferation inhibition potentials [Fig. 6 (A)]. Unexpectedly, also the empty nanoemulsion displayed a modulative effect on MYC expression leading to higher protein levels in SW480 and lower levels in K562 and MOLT4 [Fig. 6 (B)], although cell proliferation rates were almost unaffected [Fig. 6 (A)]. The reason for this effect is yet not known and requires further investigations including the analysis of other cancer signalling proteins. Furthermore, the strong reduction of cell proliferation in leukaemia cell lines after nanoemulsion-packaged peptide delivery also led to a reduction of tubulin α expression, which was used as a protein loading control [Fig. 6 (B)]. Due to these limitations, an alternative method to measure the effect of the Myr-NT peptide on MYC expression was needed. For this reason, the free BASP1 ED peptide was introduced into SW480 cells by electroporation and MYC protein expression analysed subsequently [Fig. 6 (C)]. In this case, the presence of Myr-NT led to a significant reduction in cell proliferation and a measurable reduced MYC protein expression thereby suggesting that the BASP1 ED suffices to decrease MYC protein stability as observed previously with the full-length BASP1 protein [11]. To investigate if nanoemulsions containing the BASP1-specific peptide also interfere with the known invasive property of MOLT4 cells [50], treated cells were subjected to a cell invasion assay. In contrast to adherently invasive growing cells, which remain attached after crossing an artificial extracellular membrane (ECM), tumor cells grown in suspension move

into the medium serving as an attractant. Whereas cells treated with the empty nanoemulsion efficiently passed the ECM, F2-MNT-treated cells were severely impaired in their invasive property [Fig. 6 (D)]. As activation of invasion and metastasis is one of the ten cancer hallmarks [51], inhibition of this important feature by the applied peptide-formulation also suggests a strong anti-tumorigenic effect.

3.6. Confocal laser scanning microscopy

CLSM was carried out to investigate cellular uptake of native Myr-NT-TAMRA compared with F2-MNT, complementary to the results of the biological assays. In order to get more insights into the fate of the nanoemulsion after cellular internalisation, the oily phase was additionally labelled with LGY. As LGY exhibits a logP of 7.48, it remains in the oily phase and can serve as a tracer for the lipid matrix [52], allowing to assess biodistribution of the nanoemulsion and the peptide separately. Fluorescence spectra of Myr-NT-TAMRA after HIP formation and loading into SEDDS are available in Supplementary Material Fig. S3.

Representative CLSM images and 3D models of SW480 cells after incubation with Myr-NT-TAMRA or F2-MNT are depicted in Fig. 7 (A). After incubation with the native peptide, a weak fluorescence signal could be detected inside the cells, which indicates low cellular internalisation. However, the internal fluorescence signal increased tremendously after application of the F2-MNT formulation. The average fluorescence intensities in the TAMRA channel are shown in Fig. 7 (B) and were determined to be 15-fold increased in case of SW480, and 13-fold higher for K562 and MOLT4, compared to the native peptide. A sketch of the theoretical model used for the calculation of the average fluorescence intensity is visualized in Fig. 7 (C). The data provide clear evidence on the enhanced cellular uptake of Myr-NT-TAMRA via delivery as nanoemulsion, as the amount of labelled peptide applied was identical in the formulation and the peptide reference. This is in accordance with the results of the cellular proliferation assay, in which mild biologic effects were observed on the cells after application of native Myr-NT-TAMRA, whereas pronounced anti-proliferative effects were obtained for treatment with F2-MNT.

Furthermore, the presence of the lipid matrix of F2-MNT inside the cells was confirmed by the detected fluorescence signal of LGY. The colocalization of the fluorescence signals (yellow: LGY; red: TAMRA) were 7 % for SW480, 13 % for K562 and 27 % in the case of MOLT4. This means that the majority of the incorporated peptide is successfully released from F2-MNT following cellular internalisation. Subsequently, Myr-NT-TAMRA is distributed effectively inside the cell, extending even to the nucleus, and causing the desired biologic effect, whereas the empty nanoemulsion droplets tend to form larger lipid-aggregates, which are shown in Fig. 8 (A). Interestingly, delivery via F2-MNT also led to a higher dispersal of Myr-NT-TAMRA throughout the cell, which is highlighted by finer particulate structures compared to the fluorescent clusters observed for the native peptide Fig. 8 (B).

4. Conclusion

To effectively inhibit or severely attenuate oncogenic transcription factors such as MYC in cancer cells, appropriate strategies are required

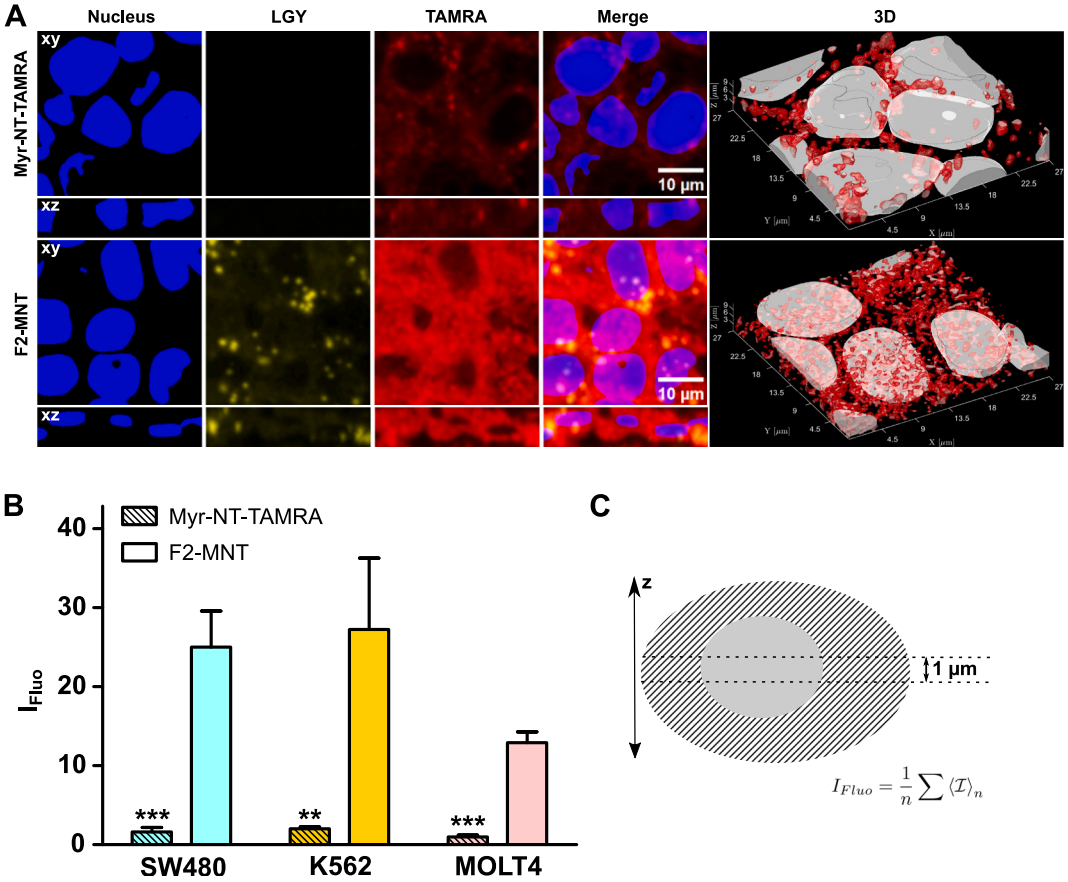

Fig. 7. CLSM images of SW480 cells after cellular internalisation of Myr-NT-TAMRA and F2-MNT **(A)**. Blue: Nucleus, Yellow: LGY, Red: TAMRA. Corresponding 3D models on the right visualize the distribution of TAMRA-peptide (red) throughout the cells and their nuclei (gray).
Average fluorescence intensity of TAMRA marker in SW480 (turquoise), K562 (orange) and MOLT4 (pink) after application of native Myr-NT-TAMRA (striped bars) and F2-MNT (bars) **(B)**. Data are means ± standard deviation of at least three experiments. Significant differences are indicated as $^{**}p < 0.01$, $^{***}p < 0.001$. Sketch of the theoretical model that was applied for determination of I_{Fluo} **(C)**. (For interpretation of the references to colour in this figure legend, the reader is referred to the web version of this article.)

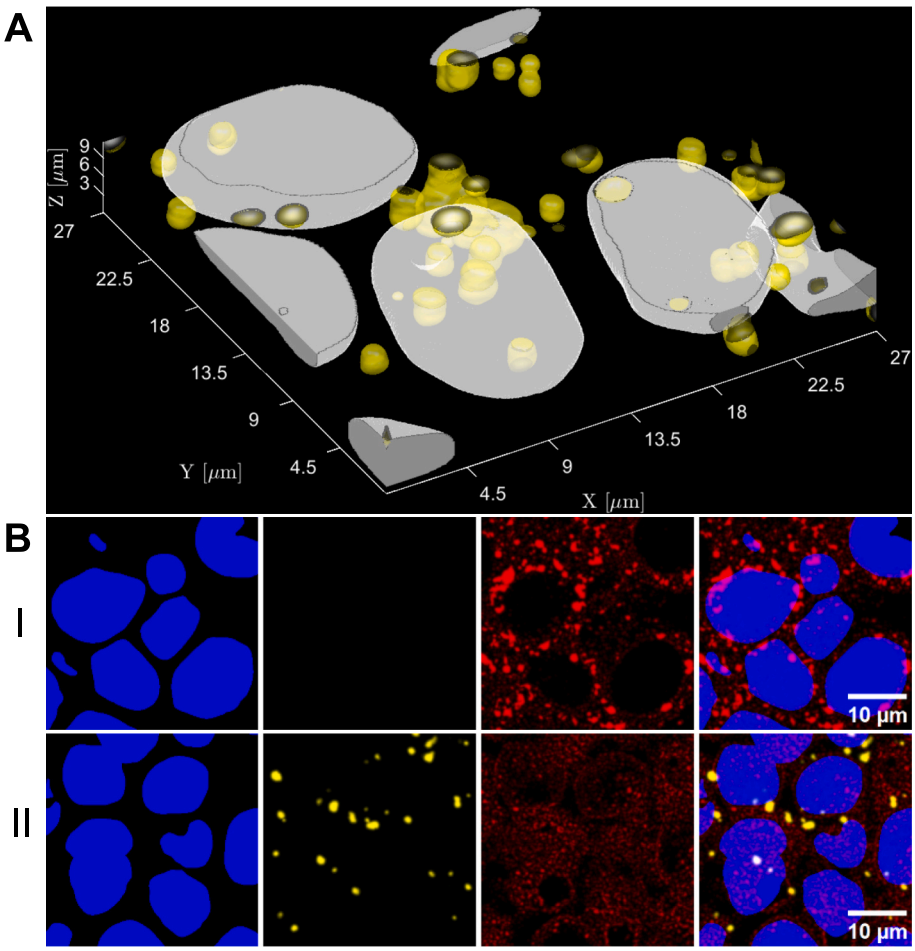

Fig. 8. Translucent 3D projection of lipid agglomerates (yellow) after cellular internalisation in SW480 cells **(A)**. Gray: Nucleus, Yellow: LGY.
CLSM images of SW480 cells after application of the native peptide Myr-NT-TAMRA **(I)** and F2-MNT **(II)** with a focus on dispersion of the TAMRA-peptide after internalisation **(B)**. Blue: Nucleus, Yellow: LGY, Red: TAMRA. To segment particulate structure a suitable threshold (algorithm: maximum entropy) was applied that led to the cut-off of parts of the fluorescence signal. In this case, even smaller, finer structures (particularly present in **II**) were excluded due to the used threshold. (For interpretation of the references to colour in this figure legend, the reader is referred to the web version of this article.)

for direct or indirect interference with the functions of these aberrantly activated gene regulators. This needs to be accompanied by the development of advanced carrier systems for effective delivery of inhibitory molecules into the target cells. Apart from the development of an appropriate inhibitor, the design of a suitable pharmaceutical formulation for specific delivery represents a prerequisite to precisely treat for instance MYC-dependent cancers. In this work, the innovative BASP1-effector peptide Myr-NT was successfully encapsulated in a lipid-based formulation purposed for oral delivery, providing significant protection against rapid inactivation by gastrointestinal proteases.

Furthermore, the nanoemulsion was able to enhance cellular internalisation and drug distribution of Myr-NT in various MYC-dependent cancer lines, resulting in ameliorated reductions in carcinogenic proliferation and cell invasion as biological response. Most importantly, there was a clear effect on adherently growing colorectal cancer cells, which represent a primary target upon oral delivery and gastrointestinal passage. Strikingly, the inhibitory effect was even more pronounced in lymphoma cells, and thus extending possible applications of our nanoemulsion beyond oral delivery.

To the best of our knowledge, this work conclusively demonstrated the efficient intracellular delivery of an anti-proliferative peptide via SEDDS and the preserved functional activity of the peptide post-delivery, assumingly evading lysosomal inactivation, for the first time. The developed formulation could therefore prospectively pave the way for the topical treatment of MYC-dependent gastrointestinal tumors via oral administration of Myr-NT after having applied appropriate in vivo tumor model systems. In the case of gastric cancer, SEDDS could be administered in the form of soft gelatin capsules that dissolve in the stomach or can be incorporated into mesoporous silica and compressed into tablets. For colorectal cancer, however, such solid dosage forms must be coated with polymers like galactomannan, ensuring targeted self-emulsification directly at the site of degenerated cells.

CRediT authorship contribution statement

Dennis To: Writing – review & editing, Writing – original draft, Visualization, Methodology, Investigation, Conceptualization. **Christian Steinbring:** Writing – original draft, Visualization, Methodology, Investigation. **Leonie I. Weber:** Visualization, Methodology, Investigation. **Fabrizio Ricci:** Methodology, Investigation. **Ilaria Polidori:** Methodology, Investigation. **Annika Postina:** Investigation, Methodology. **Markus Hartl:** Writing – review & editing, Writing – original draft, Visualization, Supervision, Methodology, Investigation, Funding acquisition, Conceptualization. **Andreas Bernkop-Schnürch:** Writing – review & editing, Supervision, Funding acquisition, Conceptualization.

Acknowledgments

The authors would like to thank Mariana Blanco Massani and Kane Puglisi for providing skilful technical assistance. This research was

supported by Austrian Science Fund (FWF) grant P33662 (to M.H.), and by University of Innsbruck Early Stage Funding (to L.I.W.)

Appendix A. Supplementary data

Supplementary data to this article can be found online at https://doi.org/10.1016/j.jconrel.2025.113677.

Data availability

Data will be made available on request.

References

[1] M.W. Berchtold, A. Villalobo, The many faces of calmodulin in cell proliferation, programmed cell death, autophagy, and cancer, Biochim. Biophys. Acta 2014 (1843) 398–435.
[2] M. Gabay, Y. Li, D.W. Felsher, MYC activation is a hallmark of cancer initiation and maintenance, Cold Spring Harb. Perspect. Med. 4 (2014).
[3] C.V. Dang, Gene regulation: fine-tuned amplification in cells, Nature 511 (2014) 417–418.
[4] E. Stefan, K. Bister, MYC and RAF: key effectors in cellular signaling and major drivers in human cancer, Curr. Top. Microbiol. Immunol. 407 (2017) 117–151.
[5] C.V. Dang, E.P. Reddy, K.M. Shokat, L. Soucek, Drugging the 'undruggable' cancer targets, Nat. Rev. Cancer 17 (2017) 502–508.
[6] M. Conacci-Sorrell, L. McFerrin, R.N. Eisenman, An overview of MYC and its interactome, Cold Spring Harb. Perspect. Med. 4 (2014) a014357.
[7] A. Baluapuri, E. Wolf, M. Eilers, Target gene-independent functions of MYC oncoproteins, Nat. Rev. Mol. Cell Biol. 21 (2020) 255–267.
[8] C. Lourenco, D. Resetca, C. Redel, P. Lin, A.S. MacDonald, R. Ciaccio, T.M. G. Kenney, Y. Wei, D.W. Andrews, M. Sunnerhagen, C.H. Arrowsmith, B. Raught, L. Z. Penn, MYC protein interactors in gene transcription and cancer, Nat. Rev. Cancer 21 (2021) 579–591.
[9] L.I. Weber, M. Hartl, Strategies to target the cancer driver MYC in tumor cells, Front. Oncol. 13 (2023) 1142111.
[10] D. Masso-Valles, M.E. Beaulieu, L. Soucek, MYC, MYCL, and MYCN as therapeutic targets in lung cancer, Expert Opin. Ther. Targets 24 (2020) 101–114.
[11] M. Hartl, K. Puglisi, A. Nist, P. Raffeiner, K. Bister, The brain acid-soluble protein 1 (BASP1) interferes with the oncogenic capacity of MYC and its binding to calmodulin, Mol. Oncol. 14 (2020) 625–644.
[12] S. Maekawa, M. Maekawa, S. Hattori, S. Nakamura, Purification and molecular cloning of a novel acidic calmodulin binding protein from rat brain, J. Biol. Chem. 268 (1993) 13703–13709.
[13] M. Matsubara, T. Nakatsu, H. Kato, H. Taniguchi, Crystal structure of a myristoylated CAP-23/NAP-22 N-terminal domain complexed with Ca2+/ calmodulin, EMBO J. 23 (2004) 712–718.
[14] A. Takasaki, N. Hayashi, M. Matsubara, E. Yamauchi, H. Taniguchi, Identification of the calmodulin-binding domain of neuron-specific protein kinase C substrate protein CAP-22/NAP-22. Direct involvement of protein myristoylation in calmodulin-target protein interaction, J. Biol. Chem. 274 (1999) 11848–11853.
[15] M. Hartl, R. Schneider, A unique family of neuronal signaling proteins implicated in oncogenesis and tumor suppression, Front. Oncol. 9 (2019) 289.
[16] L.M. Green, K.J. Wagner, H.A. Campbell, K. Addison, S.G. Roberts, Dynamic interaction between WT1 and BASP1 in transcriptional regulation during differentiation, Nucleic Acids Res. 37 (2009) 431–440.
[17] M. Hartl, A. Nist, M.I. Khan, T. Valovka, K. Bister, Inhibition of Myc-induced cell transformation by brain acid-soluble protein 1 (BASP1), Proc. Natl. Acad. Sci. USA 106 (2009) 5604–5609.
[18] P. Raffeiner, A. Schraffl, T. Schwarz, R. Rock, K. Ledolter, M. Hartl, R. Konrat, E. Stefan, K. Bister, Calcium-dependent binding of Myc to calmodulin, Oncotarget 8 (2017) 3327–3343.
[19] A. Lopalco, N. Denora, Nanoformulations for drug delivery: safety, toxicity, and efficacy, in: O. Nicolotti (Ed.), Computational Toxicology: Methods and Protocols, Springer New York, New York, NY, 2018, pp. 347–365.
[20] G. Hetényi, J. Griesser, M. Moser, F. Demarne, V. Jannin, A. Bernkop-Schnürch, Comparison of the protective effect of self-emulsifying peptide drug delivery systems towards intestinal proteases and glutathione, Int. J. Pharm. 523 (2017) 357–365.
[21] D. Stengel, B.H. Demirel, P. Knoll, M. Truszkowska, F. Laffleur, A. Bernkop-Schnürch, PEG vs. zwitterions: how these surface decorations determine cellular uptake of lipid-based nanocarriers, J. Colloid Interface Sci. 647 (2023) 52–64.
[22] S. Haddadzadegan, F. Dorkoosh, A. Bernkop-Schnürch, Oral delivery of therapeutic peptides and proteins: technology landscape of lipid-based nanocarriers, Adv. Drug Deliv. Rev. 182 (2022) 114097.
[23] A. Mahmood, A. Bernkop-Schnürch, SEDDS: a game changing approach for the oral administration of hydrophilic macromolecular drugs, Adv. Drug Deliv. Rev. 142 (2019) 91–101.
[24] R. Wibel, J.D. Friedl, S. Zaichik, A. Bernkop-Schnürch, Hydrophobic ion pairing (HIP) of (poly)peptide drugs: benefits and drawbacks of different preparation methods, Eur. J. Pharm. Biopharm. 151 (2020) 73–80.
[25] J. Griesser, G. Hétenyi, M. Moser, F. Demarne, V. Jannin, A. Bernkop-Schnürch, Hydrophobic ion pairing: key to highly payloaded self-emulsifying peptide drug delivery systems, Int. J. Pharm. 520 (2017) 267–274.
[26] H. Schagger, Tricine-SDS-PAGE, Nat. Protoc. 1 (2006) 16–22.
[27] A.M. Jörgensen, P. Knoll, S. Haddadzadegan, H. Fabian, A. Hupfauf, R. Gust, R. Georg Jörgensen, A. Bernkop-Schnürch, Biodegradable arginine based steroid-surfactants: cationic green agents for hydrophobic ion-pairing, Int. J. Pharm. 630 (2023).
[28] A. Karabasz, K. Szczepanowicz, A. Cierniak, J. Bereta, M. Bzowska, In vitro toxicity studies of biodegradable, polyelectrolyte nanocapsules, Int. J. Nanomedicine 13 (2018) 5159–5172.
[29] C. Eichler, M. Himmelstoss, R. Plangger, L.I. Weber, M. Hartl, C. Kreutz, R. Micura, Advances in RNA labeling with trifluoromethyl groups, Chemistry 29 (2023) e202302220.
[30] A.M. Jörgensen, C. Steinbring, D. Stengel, D. To, P. Schmid, A. Bernkop-Schnürch, Self-emulsifying drug delivery systems (SEDDS) containing reverse micelles: advanced oral formulations for therapeutic peptides, Adv. Healthc. Mater. 12 (2023) e2302034.
[31] J. M.A.J. Kim, Y. Kim, J.H. Jin, S.S. Kim, R.H. Kang, D. Kim, TAMRA-conjugated DRL tripeptide for the visualization of synovium, Dyes Pigments 205 (2022) 110590.
[32] K.D. Ristroph, R.K. Prud'homme, Hydrophobic ion pairing: encapsulating small molecules, peptides, and proteins into nanocarriers, Nanoscale Adv. 1 (2019) 4207–4237.
[33] V. Claus, M. Sandmeier, N. Hock, H. Spleis, S. Lindner, M. Kalb, A. Bernkop-Schnürch, Counterion optimization for hydrophobic ion pairing (HIP): unraveling the key factors, Int. J. Pharm. 647 (2023) 123507.
[34] S. Haddadzadegan, D. To, A. Matteo Jörgensen, R. Wibel, F. Laffleur, A. Bernkop-Schnürch, Comparative analysis of PEG-free and PEG-based self-emulsifying drug delivery systems for enhanced oral bioavailability of therapeutic (poly) peptides, Small 20 (2024) 2307618.
[35] R. Wibel, P. Knoll, B. Le-Vinh, G. Kali, A. Bernkop-Schnürch, Synthesis and evaluation of sulfosuccinate-based surfactants as counterions for hydrophobic ion pairing, Acta Biomater. 144 (2022) 54–66.
[36] A. Bernkop-Schnürch, A. Jalil, Do drug release studies from SEDDS make any sense? J. Control. Release 271 (2018) 55–59.
[37] M. Manaargadoo-Catin, A. Ali-Cherif, J.L. Pougnas, C. Perrin, Hemolysis by surfactants-a review, Adv. Colloid Interf. Sci. 228 (2016) 1–16.
[38] S. A.A.K. Rebello, S. Mundayoor, M.S. Jisha, Surfactants: toxicity, remediation and green surfactants, Environ. Chem. Lett. 12 (2014) 275–287.
[39] V. Claus, H. Spleis, C. Federer, K. Zöller, R. Wibel, F. Laffleur, C. Dumont, P. Caisse, A. Bernkop-Schnürch, Self-emulsifying drug delivery systems (SEDDS): in vivo-proof of concept for oral delivery of insulin glargine, Int. J. Pharm. 639 (2023) 122964.
[40] K. Zöller, F. Laffleur, V. Claus, P. Knoll, D. To, A. Bernkop-Schnürch, Development and in vivo evaluation of nanoemulsions for oral delivery of low molecular weight heparin, J. Drug Deliv. Sci. Technol. 86 (2023) 104686.
[41] P. G.B. Winkelmeier, T. Lindl, Quantification of cytotoxicity by cell volume and cell proliferation, Altern. Lab. Anim 21 (1993) 269–280.
[42] R. Perez-Roses, E. Risco, R. Vila, P. Penalver, S. Canigueral, Antioxidant activity of Tween-20 and Tween-80 evaluated through different in-vitro tests, J. Pharm. Pharmacol. 67 (2015) 666–672.
[43] R.H. Du, Y.B. Tang, J.G. Zhou, Y.Y. Guan, Effects of Tween 80 on volume-regulated chloride channel and cell proliferation in rat basilar artery smooth muscle cell, J. Pharm. Pharmacol. 63 (2011) 253–260.
[44] K. Prabst, H. Engelhardt, S. Ringgeler, H. Hubner, Basic colorimetric proliferation assays: MTT, WST, and resazurin, Methods Mol. Biol. 1601 (2017) 1–17.
[45] S. Balog, M.S. de Almeida, P. Taladriz-Blanco, B. Rothen-Rutishauser, A. Petri-Fink, Does the surface charge of the nanoparticles drive nanoparticle-cell membrane interactions? Curr. Opin. Biotechnol. 87 (2024) 103128.
[46] O. Zupančič, A. Partenhauser, H.T. Lam, J. Rohrer, A. Bernkop-Schnürch, Development and in vitro characterisation of an oral self-emulsifying delivery system for daptomycin, Eur. J. Pharm. Sci. 81 (2016) 129–136.
[47] G. Leonaviciute, O. Zupančič, F. Prüfert, J. Rohrer, A. Bernkop-Schnürch, Impact of lipases on the protective effect of SEDDS for incorporated peptide drugs towards intestinal peptidases, Int. J. Pharm. 508 (2016) 102–108.
[48] M.K. Marschütz, A. Bernkop-Schnürch, Oral peptide drug delivery: polymer-inhibitor conjugates protecting insulin from enzymatic degradation in vitro, Biomaterials 21 (2000) 1499–1507.
[49] T.N.Q. Phan, I. Shahzadi, A. Bernkop-Schnürch, Hydrophobic ion-pairs and lipid-based nanocarrier systems: the perfect match for delivery of BCS class 3 drugs, J. Control. Release 304 (2019) 146–155.
[50] G. Li, L. Gao, J. Zhao, D. Liu, H. Li, M. Hu, LncRNA ANRIL/miR-7-5p/TCF4 axis contributes to the progression of T cell acute lymphoblastic leukemia, Cancer Cell Int. 20 (2020).
[51] D. Hanahan, R.A. Weinberg, Hallmarks of cancer: the next generation, Cell 144 (2011) 646–674.
[52] J.D. Friedl, C. Steinbring, S. Zaichik, N.N. Le, A. Bernkop-Schnürch, Cellular uptake of self-emulsifying drug-delivery systems: polyethylene glycol versus polyglycerol surface, Nanomedicine (London) 15 (2020) 1829–1841.